October 2021

Synthesis of Functionalized Acrylic Nanoparticles as a Precursor to Bifunctional Colloids

Guinevere E. Tillinghast
University of Massachusetts Amherst

Synthesis of Functionalized Acrylic Nanoparticles as a Precursor to Bifunctional Colloids

Guinevere E. Tillinghast

SYNTHESIS OF FUNCTIONALIZED ACRYLIC NANOPARTICLES AS A PRECURSOR TO BIFUNCTIONAL COLLOIDS

A Thesis Presented

by

GUINEVERE TILLINGHAST

Submitted to the Graduate School of the

University of Massachusetts Amherst in partial fulfillment

of the requirements for the degree of

Master of Science in Chemical Engineering

September 2021

Chemical Engineering

SYNTHESIS OF FUNCTIONALIZED ACRYLIC NANOPARTICLES AS A PRECURSOR TO BIFUNCTIONAL COLLOIDS

A Thesis Presented

by

GUINEVERE TILLINGHAST

Approved as to style and content by:

_____

John Klier, Co-Chair

_____

Peter J. Beltramo, Co-Chair

_____

Jessica D. Schiffman, Member

_____

H. Henning Winter, Member

_____

Laura C. Bradley, Member

_____

Michael Henson, Department Head

Chemical Engineering

ABSTRACT

SYNTHESIS OF FUNCTIONALIZED ACRYLIC NANOPARTICLES AS A PRECURSOR TO BIFUNCTIONAL COLLOIDS

SEPTEMBER 2021

GUINEVERE TILLINGHAST, B.S., RENSSELAER POLYTECHNIC INSTITUTE

M.S.Ch.E., UNIVERSITY OF MASSACHUSETTS AMHERST

Directed by: Professor John Klier and Professor Peter J. Beltramo

Water-borne coatings have increased in popularity due to the recent environmental regulations being placed on coating formulation. The most readily available coatings without volatile organic compounds are thermoplastic polymer dispersions that rely on interdiffusion to form a film. These dispersions are reliant on toxic crosslinking chemistries to achieve adequate coating mechanical properties, but still have significantly inferior properties when compared with current thermosetting industrial coatings that contain volatile organic compounds. As a result, waterborne coatings made with conventional emulsion polymers cannot be considered for high-performance coatings. Polyurethane dispersions have been developed that can meet these demands, but require several lengthy coating applications and are therefore incredibly costly. A water-based acrylic emulsion polymer coating that could self-stratify and apply multiple crosslinkable layers simultaneously, has the potential to revolutionize current coating formulations. Recent advances in anisotropic polymer colloid synthesis offer a potential pathway to make such a high-performance coating. Incorporating unique functionality into each of the lobes of a

bilobal particle would enable the formation of a new class of water-based, self-stratifying, high-performance, acrylic coatings.

The primary goal of this thesis was to show proof of concept for a bilobal platform that could be used to form water-based self-stratifying coatings. The approach was adapted from recent advances in pigment-associating emulsion polymers used to improve coating pigment dispersion. Butyl acrylate and methyl methacrylate seed particles ~90 nm in size were formed and subsequently used to synthesize preliminary ~130 nm acrylic bilobal particles, within the target size range of water based coating dispersions. Control over the seed particle glass transition temperature, size, and morphology, and synthesis of promising preliminary bilobal particles was demonstrated; this was accomplished using a systematic analysis of various reaction conditions, namely, pre-emulsification, reaction duration, and the concentrations of the monomers. Expanding upon the chemical versatility would enable these particles to be used in a wide variety of applications, but this thesis represents a promising start for the bilobal platform within the coating industry.

TABLE OF CONTENTS

LIST OF TABLES

LIST OF FIGURES

CHAPTER 1

INTRODUCTION

1.1 Current State of Commercial Coating Market

1.1.1. Waterborne Coatings

Waterborne coatings, powder coatings and other high-solids formulations are increasing in popularity as environmental regulations on coating formulations become more stringent. These products aim to replace existing mainstream formulations that rely on solvents to achieve low cost, high-quality coatings.[1,2] Solvents "soften" the individual polymers, prevent aggregation, and facilitate film formation by allowing the polymers to flow into a coherent film before crosslinking to each other. Crosslinking is often necessary for the coating to stand up the mechanical properties required for high-performance industrial applications such as automotive or architectural coatings. However, during solvent evaporation hazardous volatile organic compounds (VOCs) are released. Alternative methods of durable film formation are necessary for low-VOC and zero-VOC products to match the performance of solvent-borne systems.[1,2]

Most water-borne coatings are thermoplastic dispersions comprised of acrylic, acrylic-styrene, or vinyl acetate produced via free radical emulsion polymerization. These materials cannot be crosslinked prior to application because the polymers need to flow and coalesce while the water is evaporating. The most common approach to improve these coatings is to incorporate a supplemental crosslinking agent.[3] Popular crosslinking agents are poly-aziridines, poly-carbodiimides, and poly-isocyanates; however, all three chemistries are highly toxic.[4] These crosslinking agents are mixed in with the emulsion

polymers immediately before application onto the substrate and crosslinking is triggered by the evaporation of the water. Acetoacetoxy ethyl methacrylate is another crosslinking agent that can be incorporated into the initial formulation without the need for a separate processing step. For all of these chemistries, the extent of crosslinking and improvement of the mechanical properties is minimal and, as a result, these coatings cannot be used for high-performance industrial applications. In principle, a higher level of performance could be achieved by incorporating high levels of crosslinkable double bonds directly into the polymers. The film would then be initiated by an additional processing step, such as high temperature baking or UV. However, this approach is not currently available for conventional emulsion polymers because the double bonds are consumed by free radical polymerization. Methods of crosslinking that do not rely on toxic chemistries, and ideally are UV initiated, continue to be of significant interest to the coating industry.

Polyurethane dispersions (PUDs) are the most readily available waterborne coating resins that are not formed via free radical polymerization. PUDs are instead formed by reacting a polyol with a diisocyanate or a polymeric isocyanate. This allows the PUDs to be loaded up with double bonds for convenient and powerful free radical crosslinking after application. It should be noted, a disadvantage of PUDs is that these poly-isocyanates are highly toxic while in an uncured state, this includes manufacturing and application; PUDs are non-toxic in a dried state because the poly-isocyanates hydrolyze. There are several advantages when considering PUDs: they have high molecular weights and mechanical strength, but also feature softer domains to allow movement of the polymers into a smooth surface.[5] In addition to toxicity concerns, drawbacks of PUDs are that they are costly, have long application times, and in most cases are limited to application of a single-layer at a

time. Waterborne self-priming or self-stratifying PUDs formulations are rare, as a result, to achieve additional functionality or increased thicknesses, the coating requires multiple coats and many drying and curing steps.

Research into water-borne polymers using more cost effective materials is ongoing, commercial hybrid urethane/acrylate systems have already been successful.[2] Recent epoxy[6] and polyolefin[7] coatings are promising but lack durability and often degrade under UV exposure, as a result these formulations represent only a small portion of the coating market.[4] Acrylic polymers are durable and resistant to degradation from UV, heat, and alkalinity, and are highly cost effective. As previously described, however, current waterborne acrylic coatings are inadequate for many high-performance coatings.

1.1.2. Self-Priming and Self-Stratifying Coatings

Single layer coatings, such as the previously described waterborne PUDs, are often unable to meet the demands for high-performance automotive and architectural coatings, necessitating the development of multi-layer and multi-functionality coatings. Typically, multilayer coatings consist of a bottom primer layer, an application specific core layer, and a topcoat **(Fig. 1).** Application requires separate processing steps with long curing times and high labor costs overall. Each layer has a unique formulation and separation at the interphase between the layers can occur, reducing the quality and performance. The primer layer allows for adhesion of the substrate, while the topcoat provides weatherability and

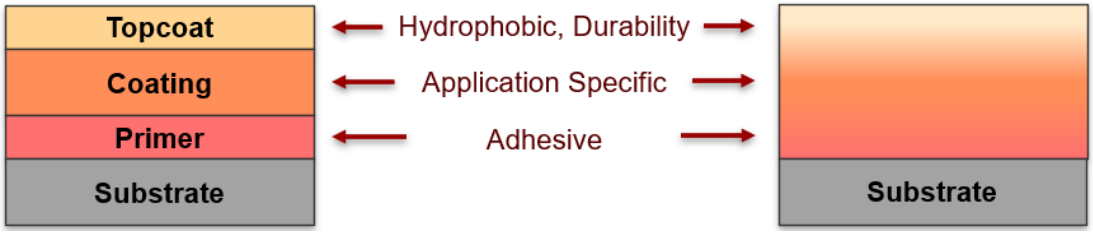

Figure 1: Comparison of multi-layer and self-stratifying coatings, adapted from Beaugenre et al.[9]

resistance to UV, abrasion, and hydrolysis. Significant interest has been placed in self-priming and stratifying coatings which are designed to apply multiple layers at a time.[8,9]

Self-stratifying coatings have been investigated for a wide variety of materials, such as, acrylic,[10] epoxy,[8] polyurethane,[11] and silicone.[12] However, all of these examples still rely either fully or partially on solvents, which are necessary enable the movement of the polymers into the desired configuration **(Fig. 2)**. The critical factors that contribute to the success of stratification are currently being investigated and optimized, these include solvent volatility, resin surface energy and polarity, curing temperature, and crosslinking reactivity.[11] While these examples are promising advancements, there remains a need for fully water based cost effective self-stratifying coating technologies.

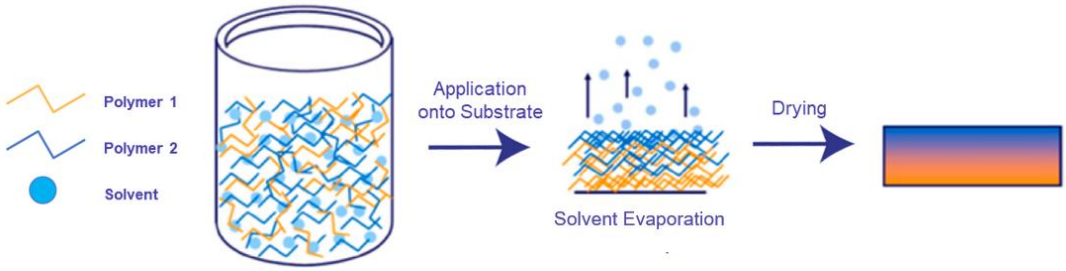

Figure 2: How solvent evaporation drives self-stratification, adapted from Beaugenre et al.[9]

1.2. Evaluation of Bilobal Particle Synthesis Procedures

Recent advances in anisotropic polymer colloid synthesis offer a potential pathway to water-based self-stratifying high-performance acrylic coatings. By introducing a second polymerization step to spherical seed particles, bilobal particles may be formed.[13–21] Unfunctionalized bilobal particles have already garnered significant interest.[18,21,22] Incorporating unique functionality into each of the lobes would enable the particles to be used in a wider diversity of applications including a new class of high-performance coatings. For example, we propose the use of bilobal particles in self-stratifying coating

applications where one lobe functionality would include an adhesive moiety, while the other can be the chemistry of interest. In this manner, a bilobal suspension may self-assemble onto solid surfaces with the desired morphology and chemistry.

Bilobal particles can be generated for a variety of morphologies such as acorn, hemisphere, or dumbbell **(Fig. 3)**. These systems can also be referred to as Janus particles when there are two unique surfaces on the same particle, such as a material or functionality difference. There are two primary methods of bilobal particle synthesis, one method involves swelling the second phase within the initial seed particle[13–19] and the alternative method entails coating an initial seed particle with a second polymer phase.[18–21] Either method relies on the formation of monodisperse, spherical polymer seed particles.

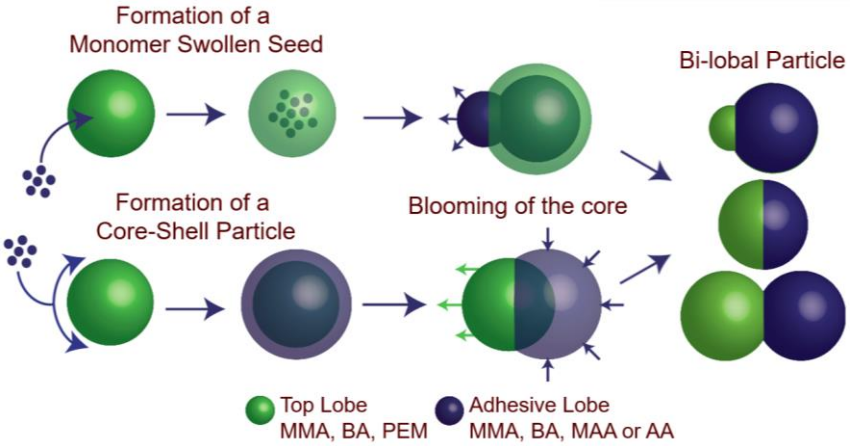

Figure 3: Overview of the two paths available for bilobal particle synthesis.

Formation of the seed particle precursor is usually via emulsion polymerization, but it should be noted that there are other routes to seed particle formation such as dispersion and suspension polymerization. The method of seed particle formation should not impact the second phase bilobal formation as long as the monomers are well distributed throughout the seed. It is important that the seed particles going into the second phase emulsion polymerization have high monodispersity and spherical morphology to produce consistent bilobal particle morphologies. A number of parameters can be used to optimize synthesis

such as the type and concentration of the surfactant, monomer, and initiator, temperature, pH, and stir rate.[23] The most common seed particles for bilobal particle synthesis are styrene or hybrid styrene and acrylics such as methyl methacrylate (MMA) and butyl acrylate (BA).

Pre-emulsification of the seed particle monomer(s) with surfactant and water allows for the formation of monomer saturated surfactant micelles prior to addition into the reactor, which can improve monomer distribution. Monomer starved conditions will also improve monomer distribution, the monomer and initiator are added linearly over a set period of time and consumed immediately, preventing build-up in the reactor. Lastly, an initiator chase where the initiator is inputted slightly longer than the monomer can help prevent residual monomer that was unreacted during the polymerization. Catalyst/activator pairs and dialysis can also be used to remove unreacted residual monomer.

The final bilobal particle morphology is dependent on several parameters, most notably, the interfacial tensions between the polymer phases and the bulk and their effect on equilibrium morphology **(Fig. 4)**.[14,18,21] Kim et al. explored this phenomena using systematic synthesis of three micron polystyrene and poly alkyl acrylate hybrid Janus particles. Polystyrene seed particles were swelled with varying alkyl acrylate chain lengths, altering medium solvency was also investigated. They found that the system will be driven to reduce the total interfacial free energy, which can be related to the interfacial tensions (γ_{ij}) and interfacial areas (S_{ij}) of the system:[14]

$$G = \gamma_{12}S_{12} + \gamma_{13}S_{13} + \gamma_{23}S_{23}$$

With seed polymer phase (1), second phase (2), and bulk (3). This equation can then be used to predict particle equilibrium morphology. When γ_{13} or γ_{23} is high a core-shell will

be formed to minimize S_{13} or S_{23} **(Fig. 4.1-4.2)**. When γ_{12} is also low, occlusions or an entirely mixed seed will form to maximize S_{12} instead of a distinct phase separated system. When γ_{13} and γ_{23} are both low it is possible to form bilobal particles **(Fig. 4.3)**, however, if γ_{12} is also high two independent seed particles can form instead. Evidently, equilibrium morphology can vary widely, thus, restricting the system from equilibrium can also be viable for synthesis.

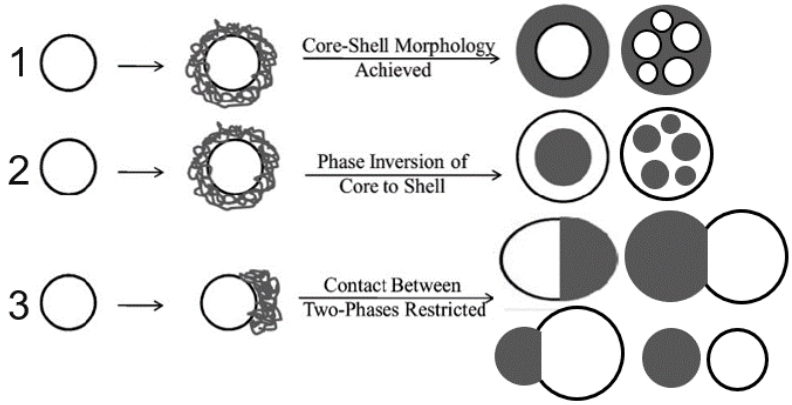

Figure 4: Core-Shell approach to form bilobal particles, equilibrium morphologies under different conditions are shown, adapted from Misra et al.[21]

The glass transition temperature (T_g) of the polymers used during bilobal particle synthesis is a critical parameter because it allows or disallows migration into the equilibrium state. T_g is the temperature when a polymer reversibly transitions between a hard, "glassy" state and a soft, "rubbery" state. At temperatures above a polymer's T_g it will behave more viscously, below the T_g the polymers will have limited mobility. Monomers can be classified into soft, medium, and hard categories based on the T_g of their homopolymer. Stubbs et al. investigated the effect of reaction temperature, relative to T_g, on systems with different equilibrium morphologies and created a decision tree flow chart that could predict the final particle morphology **(Fig. 5)**.[18] During synthesis, if the reaction temperature is below the T_g of the seed particle, the equilibrium can be restricted because the reacting oligomers becoming entangled if they try to enter the seed particle.

Entanglement can also occur for certain monomer compositions, such as acrylics, or when crosslinking of the seed particle is present. This can force the system into a core-shell configuration even if the equilibrium morphology is not core-shell **(Fig. 5.1-5.3)**.[18,21]

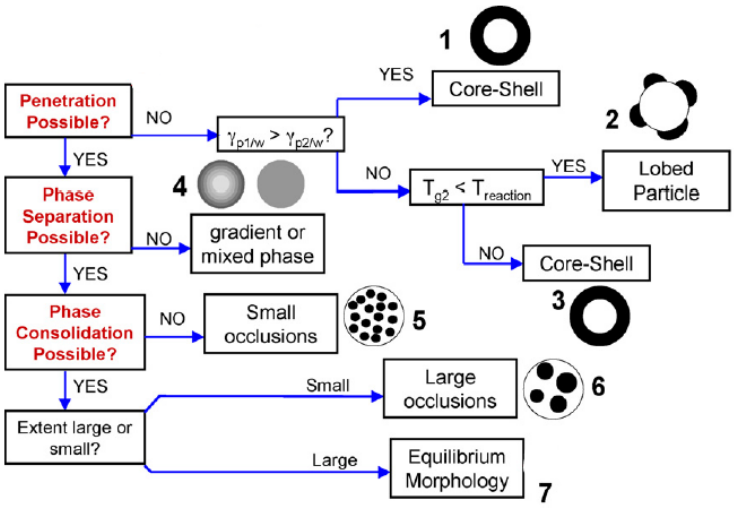

Figure 5: Decision tree flow chart by Stubbs et al. to predict bilobal particle morphology.[18]

Restricting the system from achieving its equilibrium morphology can be used to generate bilobal particles. The decision tree flow chart by Stubbs et al. was used to inform the optimization of their synthesis of MMA, methyl acrylate, styrene, and hexyl methacrylate hybrid Janus particles **(Fig. 5.2)**.[19] These particles are of an ideal size range for a coating application, roughly 100-300 nm, but the particles have irregular morphologies. These particles were also crosslinked with ethylene glycol dimethacrylate which prevents usage in coatings because the particles would need to be crosslinked after application on a substrate.

One of the more promising approaches has been developed by Bohling, et. al., who also utilized restriction into the equilibrium morphology to form MMA, BA, styrene hybrid bifunctional particles.[20,24] The first synthesis step is the formation of a core-shell particle, in this case, the core is primarily BA and MMA and the shell is primarily BA and styrene.

"Blooming of the core" is then initiated via the addition of a strong base after polymerization is completed **(Fig. 3)**. Surface functionalization was incorporated using functional monomers, phosphoethyl methacrylate (PEM) and carboxylic groups from methacrylic acid (MAA) or acrylic acid (AA). This innovative approach is a promising method of controllable synthesis of bifunctional bilobal particles.

Incorporation of functionality into bilobal particles has been investigated extensively, however, bifunctionality is a feature that has proven difficult to implement in a bulk synthesis procedure. Chang et al. was able to synthesize bifunctional Janus particles by dispersion polymerization of an initial styrene seed. (2-(2-bromoisobutyryloxy) ethyl methacrylate) was used to form a brominated core-shell particle which were then swollen with propargyl acrylate and polymerized.[17] The resulting 2-3 micron Janus particles had bromide groups on one face and alkyne functionality on the other. Other bifunctional particle synthesis procedures include microfluidics[25,26] and various surface initiated synthesis procedures such as microcontact printing[27] and lithography.[28] Many of the promising functional and bifunctional particles produced are relatively large, greater than one micron. The appropriate particle size range for usage in coatings is 100-300 nm; this size range enables coalescence into a coating surface via capillary forces.[29] Additional work is necessary to make bifunctional particles that can be used within coatings.

1.3. Proposed Precursory Seeds and the Bilobal Platform

One instance of bifunctionalized bilobal particles within commercial coatings was by Bohling et al. to develop particles capable of encapsulating pigments and improve pigment spacing **(Fig. 6a)**.[20,24] One lobes of the bilobal particles are is functionalized with an adhesive lobe to bind the pigments and substrate, while the other lobe and a second contains

a functionality that is polar and repels the other encapsulated pigment particles. The particles generated by the Bohling et al. patent are of an appropriate size range and incorporate bifunctionality with a scalable bulk synthesis procedure using cheap but effective acrylic styrene chemistries.[20] However, the details of this synthesis are obfuscated by the patent and a more thorough investigation of the synthesis steps, from the seed particles to bilobal particles is necessary to apply this technique more broadly across the possible application space. Beyond this example, exploration of bifunctional particles in industrially relevant coatings is limited.

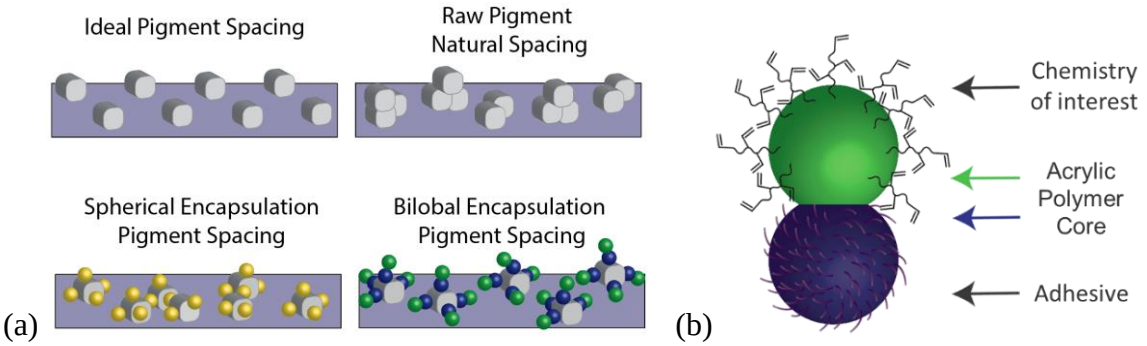

Figure 6: (a) How pigment spacing can be improved by using spherical and bilobal encapsulation, adapted from Klier et al. (b) Proposed bilobal particle platform. The green lobe will be referred to as the top lobe and the blue lobe will be called the adhesive lobe.[2]

The long term goal that this thesis will work towards is the expansion of the Bohling procedure to create a bilobal platform capable of making water-based self-stratifying acrylic coatings. The proposed platform can be divided into three distinct parts, an acrylic polymer core and two functionalized lobes referred to as the "adhesive lobe" and the "top lobe" **(Fig. 6b)**. If one lobe has a strong affinity for the substrate, relative to the other lobe, orientation can be controlled.[12] The top lobe can then be a carrier for a second functionality based on the needs of the coating. The versatility of the bilobal platform lends itself to numerous potential applications such as: pigment encapsulation,[20,30] anti-fouling coatings for biological applications,[31] catalysis,[32] and alternating refractive index optical

coatings[33,34]. The primary application of interest in this study is high-performance multilayer automotive and architectural coatings.

Within this study T_g of the seed precursors will be controlled using BA, a soft monomer with T_g -53°, and MMA, a hard monomer with T_g 105 °C. Harder monomers increase film cohesion and abrasion resistance while soft monomers improve ease of application by decreasing viscosity.[35] The two functionalities that will incorporated into the model bilobal platform are phosphate groups using phosphoethyl methacrylate (PEM) in the initial seed particles and carboxylic groups from methacrylic acid (MAA) or acrylic acid (AA) in the second phase emulsion polymerization. PEM is a particularly strong adhesive for metal substrates and has been found to improve water repellency, corrosion resistance, and abrasion resistance.[17] To enable UV-crosslinking of the final coating, carboxylic acid has been chosen due to its ability to act as a functional intermediate. The pendant carboxylic groups will also control surface polarity of the system and be a key feature in initiating the blooming of the core to form bilobal particles. In future studies, hydroxyethyl methacrylate methylene malonate (HEMA-MM), which contains UV reactive polymer chains, can be grafted to the top lobe via anionic polymerization with the carboxylic groups under ambient conditions **(Fig. 7)**.[18] This system can be used in conjunction with pre-existing spherical systems to control film thickness.

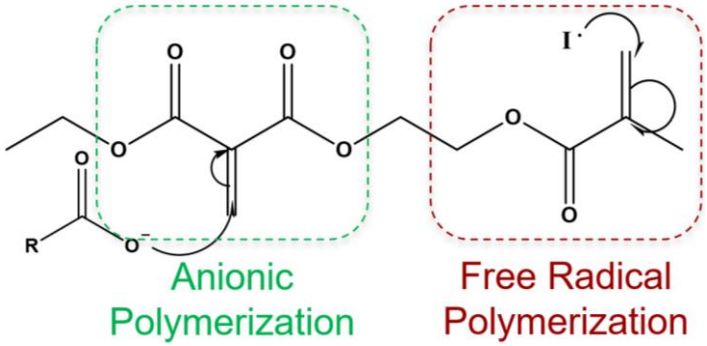

Figure 7: Chemical structure of hydroxyethyl methacrylate methylene malonate (HEMA-MM)

1.4. Study Objectives

As outlined above, there is a need for fully water-borne, self-stratifying coatings, and bilobal emulsion polymer particle synthesis offers a potential pathway. Therefore, the goal of this project is to create a foundation for a multi-functional bilobal platform that will enable efficient multilayer coating formation through chemical control of different lobes of anisotropic colloids in the future **(Fig. 3)**. Specifically, the primary objective will be to optimize seed particle synthesis and the secondary objective will be to demonstrate proof-of-concept bilobal particles with promising seed particles. Control over seed particle morphology, size, and monodispersity will be evaluated as a function of processing conditions such as pre-emulsification, reaction duration, and initial monomer concentration.

The seed particle glass transition temperature will be controlled by the overall monomer composition. Reaction conditions will be initially based on the Bohling 2015 patent[20], described above, and variations on the procedure will be used to improve the seed particles prior to the second phase emulsion polymerization. Once the ideal seed particle conditions have been determined, the second objective will be preliminary demonstration of the bilobal particle synthesis. The main parameter that will be varied to optimize the bilobal particles is the ratio between the seed particles and the second phase monomers, which controls the final particle morphology, size, and overall yield. The results of this work are a critical starting point for the further development of polymer nanoparticles with controlled bifunctionality.

CHAPTER 2

MATERIALS AND METHODS

2.1. Phase One Seed Particle Synthesis Procedure

The experimental setup can be seen in **(Fig. 8)** and the reagent masses for the control can be seen in **(Tbl. 1)**. The reagents were scaled down approximately 5x from that used in the Bohling et al. 2015 patent.[20] Individual component weight percentage is defined as mass of the reagent relative to the total mass, i.e. 23 wt% BA for the control synthesis. The total monomer weight percentage is defined as the sum of monomer masses, BA, MMA, allyl methacrylate (AMA), and MAA, relative to the total mass, i.e. 38 wt% for the control synthesis.

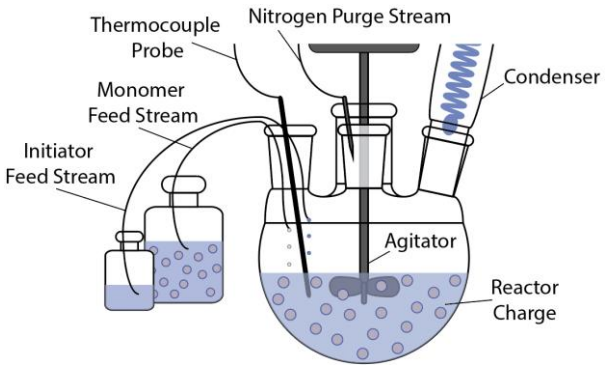

Figure 8: Four neck flask experimental set-up with condenser, thermal couple, agitator, nitrogen purge stream, and monomer/initiator feed streams. Syringe pumps not shown.

The synthesis begins by charging a four neck flask reactor with 115 mL milli-q water and sodium laureth-12-sulfate, commercially known as Disponil FES 993, acquired from BASF. Baseline reaction conditions were a stir rate of 400 rpm and a temperature of 85 °C. The monomer feed stream was pre-emulsified at 400 rpm by a magnetic stir-bar while at room temperature. The monomer pre-emulsion contains BA, MMA, AMA, MAA, PEM, Disponil, and milli-q water. Typical reaction concentrations are shown in **(Tbl. 1)**, where the BA and MMA are incorporated in a roughly 2:1 mass ratio with much smaller amounts

of PEM, MMA, and AMA. As explained later, since BA and MMA are the main components of the monomer feed, their relative concentrations will be varied in order to control the final glass transition temperature of the seed particles. The Disponil concentration in the pre-emulsion is such that 75% of the total surfactant used is in this stream, with the balance initially in the reactor charge. Sodium persulfate (NaPS) was used as the initiator and added in two successive solutions. The second initiator solution is less concentrated to maintain the initial concentration of initiator over the course of the reaction.

To begin the synthesis, the reactor is charged with a 20 mL portion of the monomer pre-emulsion and first initiator solution, the rest of the monomer pre-emulsion and the second initiator solution is then added linearly over 40 and 50 minutes, respectively. Once all of the monomer and second initiator solution are added, the reaction proceeds under an inert atmosphere, and at constant temperature (85 °C), for an additional four hours to prevent incomplete polymerization. Once this time has passed, the reactor contents are transferred into a vessel for storage and allowed to cool at room temperature.

Location	Reagent	Patent Mass (g)	300 mL Mass (g)	wt%	
Pre-Emulsion	PEM	34.1	6.69	2	38
	BA	371	72.7	23	
	MMA	195	38.2	12	
	AMA	9.6	1.88	1	
	MAA	12.8	2.51	1	
	Water	225	40	13	62
	Disponil	64	12.55	4	
Reactor	Water	600	115	36	
	Disponil	21.3	4.18	1	
Initiator 1	NaPS	2.56	0.502	-	
	Water	60	15	5	
Initiator 2	NaPS	0.64	0.125	-	
	Water	50	10	3	

Table 1: Reagents for the seed particle control synthesis based on Bohling et al. 2015 patent.[20]

2.2. Phase Two Bilobal Particle Synthesis Procedure

The same reactor set up that is used in phase one is used to create the bilobal acorn particles. The reagent masses for the control can be seen in **(Tbl. 2)**, scaled down approximately 10x from that used in the Bohling et al. 2015 patent.[20] Unlike the previous procedure, surfactant is not initially in the reactor charge and is only added with the monomer pre-emulsion stream. The baseline reaction conditions do not change; a stir rate of 400 rpm and a temperature of 85 °C are used. For phase two the monomer pre-emulsion contains BA, styrene, AA, sodium 4-vinylbenzenesulfonate (SVBS) to act as a colloidal stabilizer, sodium dodecylbenzene sulfonate surfactant (SDBS), and milli-q water. To be consistent with the initial patent procedure, vinyltrimethyoxysilane (VTMS) is also included. VTMS is listed as an optional reagent to provide hydrophobicity to the subsequent coating.

To begin the reaction the reactor is charged with a 40 mL portion of the phase one seed particles and the first initiator solution. Ammonium persulfate (NH_4PS) and sodium hydroxide (NaOH) were used in the second initiator solution to lower the pH of the system

Location	Reagent	Patent Mass (g)	300 mL Mass (g)	Wt%	
Pre-Emulsion	BA	857	86.7	26	43
	Styrene	546	55.2	16	
	AA	28.8	2.91	1	
	VTMS	4.3	0.43	-	
	SDBS	16.9	1.71	1	57
	SVBS	4.8	0.49	-	
	Water	390	40	12	
Reactor	Water	800	85	25	
	Seed Particles	400	40	12	
Initiator 1	NH_4PS	4.8	0.49	-	
	Water	25	15	4	
Initiator 2	NaPS	2.4	0.243	-	
	NaOH	2	0.2	-	
	Water	57	10	3	

Table 2: Reagents for the bilobal particle control synthesis based on Bohling et al. 2015 patent.[20]

and enable the “blooming of the core” to form bilobal particles. The second phase monomer pre-emulsion and the second initiator solution are then added linearly over 110 and 120 minutes, respectively. Once all of the monomer and second initiator solution are added, the reaction proceeds under an inert atmosphere, and at constant temperature (85 °C), for an additional four hours to prevent incomplete polymerization. Once this time has passed, the reactor contents are transferred into a vessel for storage and allowed to cool at room temperature.

2.3. Characterization Techniques

Particle size and morphology were characterized using three techniques: dynamic light scattering (DLS), scanning electron microscopy (SEM), and transmission electron microscopy (TEM). Nanoparticle samples were prepared for analysis using 5-7 days of dialysis to allow residual monomer to separate from the synthesized particles. The dialyzed samples are then diluted by a factor of 800. DLS is set up based on the translational diffusion coefficient of BA for all tests. Particle size is averaged based on 3 trials with 10 data points each, after an initial 1-minute acclimation period. The DLS polydispersity index (PDI) will be used to quantify the variability in particle size. For SEM, droplets of the dialyzed and diluted samples are placed onto copper tape and dried in a desiccator for a minimum of 24 hours. For TEM, the samples are dried in the same fashion onto a copper grid. Differential scanning calorimetry (DSC) was performed on the unprocessed samples, prior to dialysis and dilution, after drying for 24-36 hours in a vacuum oven. Samples are heated twice, with a cooling step in between, and the glass transition is determined based on the slope of the second heating curve to give each sample the same thermal history.

CHAPTER 3

RESULTS AND DISCUSSION

3.1 Seed Particle Synthesis

3.1.1 Monomer Pre-Emulsification

As a first insight into the synthesis of acrylic seed particles, we investigated the necessity of a pre-emulsification step. Pre-emulsification entails mixing water and surfactant into the monomer feed stream prior to addition into the reactor. When the pre-emulsification step is not used, the monomer feed stream contains only the monomers listed in **(Tbl. 1)** above, and the surfactant is only present in the initial reactor charge. Pre-emulsification has been shown to increase the rate of polymerization and conversion. It also extends shelf-life of the final product by reducing coagulation, and increases water repellency by lowering the necessary overall surfactant levels.[36] As a result, pre-emulsification has been widely adopted for many commercial polymerization processes; however, in certain systems it can negatively impact particle distribution.

The increase in particle distribution is due to the formation of concentrated small monomer droplets within the pre-emulsion, which are what enable the increased reaction velocity. The high surface area of the small pre-emulsified monomer droplets will directly impact the increase in reaction velocity, by enhancing the rate of transfer of monomer from the droplets into the micelles where polymerization takes place.[37] However, when the surface areas of these monomer droplets is very high, some of the radicals initiated in the aqueous phase will transfer into the droplets rather than the surfactant micelles, where polymerization normally occurs. Competition between the micelles and the monomer

droplets is what can cause broad or bimodal particle distribution.[36] When pre-emulsification is not used there will be very few monomer droplets and competition with the micellar polymerization does not occur.

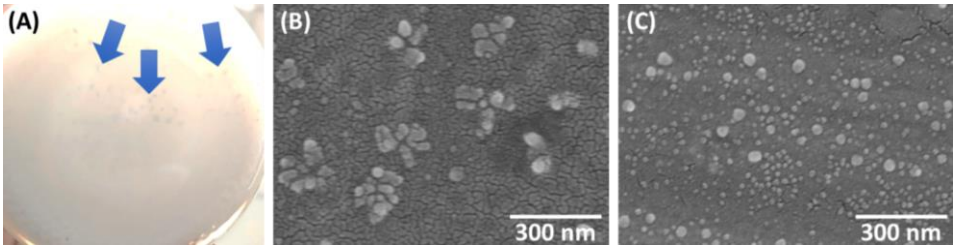

Figure 9: Evaluation of the pre-emulsification step: (A) The underside of the sample container without pre-emulsification, arrows are indicating clumps of particles, (B) SEM without pre-emulsification, and (C) SEM with pre-emulsification.

Polymerizations were performed with and without pre-emulsification to determine the effect on particle size and morphology, keeping the concentration of BA constant at 23 wt% and an overall monomer concentration of 38 wt%. As shown in **(Fig. 9a)**, significant agglomerates are visually obvious in the reactor flask after performing a synthesis without pre-emulsification step. SEM imaging of samples without pre-emulsification show the presence of large aspherical aggregates **(Fig. 9b)**, whereas once pre-emulsification is implemented the synthesized particles are spherical and not aggregated **(Fig. 9c)**. It should be noted that these polymerizations were carried out with a reduced reaction time of 1-hour, 10 minutes after the feed stream ended, rather than the typical 5-hour duration, which is discussed in the next section.

Lastly, this set of experiments also revealed the importance of having multiple means of characterizing the final particle size and morphology. DLS on both samples showed minimal difference in the measured particle diameter with pre-emulsification (103 nm) and without pre-emulsification (89 nm). The importance of pre-emulsification is likely due to the complexity of the monomer blend, which contains polar MAA and PEM and non-polar

BA, MMA, and AMA. Forming a pre-emulsion via the addition of surfactant and stirring helps prevent the polar and non-polar monomers from phase separating and encourages uniform polymerization in the reaction chamber.

For this study, the pre-emulsification conditions were a stir rate of 400 rpm using a stir bar, while at room temperature, with 75% of the total surfactant within the pre-emulsion. These conditions will be used in all experiments that follow, however, there may be an opportunity to investigate these parameters further for improved seed particle synthesis. Durbin et al. showed for a simple system using styrene, SDS, and water, increasing the intensity of mixing will decrease the average monomer droplet size.[37] With 75% of the total surfactant contained within the pre-emulsification, the number of monomer droplets will be considerably higher than without pre-emulsification.

Reducing the total surfactant within the pre-emulsification or stirring rate could be used to control the number of monomer droplets and improve particle distribution, but homogeneity of the feed stream would still need to be maintained.[36] Cui et al. found the ideal ratio for their system using BA, MMA, and AA monomers with sodium dodecyl sulfate and 2-acrylanmido-2-methylpropane sulfonic acid surfactants was between 33-66% total surfactant within the pre-emulsification.[36] It has been shown that heating the pre-emulsification is an alternative approach to increasing homogeneity in the pre-emulsion without excessive surfactant or over agitating. Chen et al. monitored pre-emulsion homogeneity by UV spectrophotometry and showed that homogeneity of styrene and AA pre-emulsions was drastically improved at temperatures above 65 °C.[38]

3.1.2 Reaction Duration

The particles generated for pre-emulsification testing had a reaction time of 1-hour, however, analysis into reactivities of acrylic monomers has shown that maximizing conversion necessitates 4+ hour reaction durations.[39] Therefore, the duration of the reaction was investigated to see the effect on particle size, T_g, and morphology. In **(Fig. 10-11)**, 1-hour and 5-hour reaction times are compared for 16 and 23 wt% BA. Stopping the reaction at 1-hour immediately after the monomer and initiator feed streams completed was found to yield smaller particles with inconsistent shape, whereas the longer reaction time produced larger particles with a more spherical morphology.

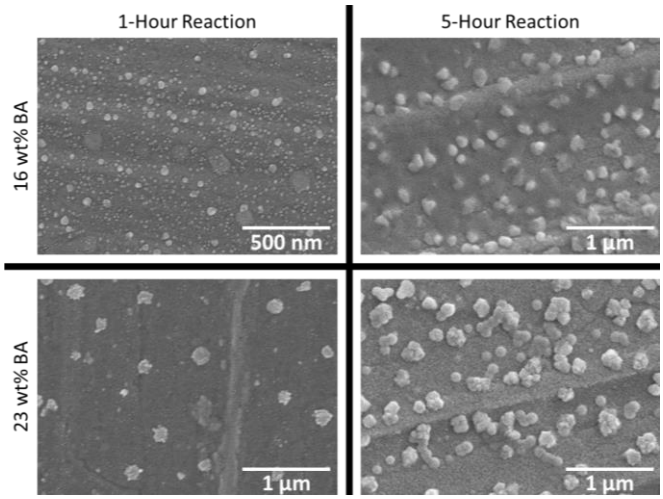

Figure 10: SEM imaging analyzing the effect of altering reaction duration from 1-5 hours, investigated for 16 and 23% wt% BA.

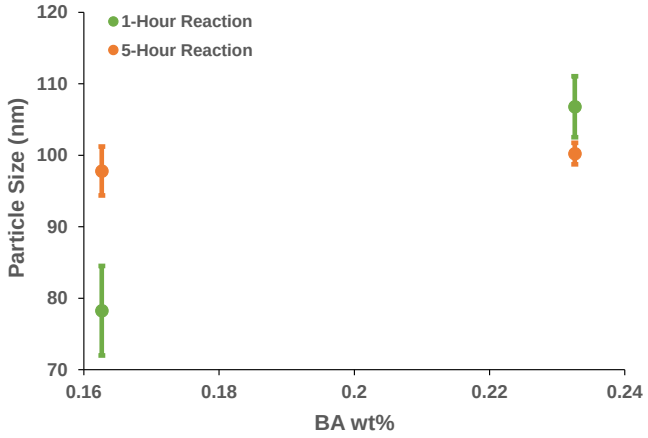

Figure 11: DLS results showing the effect of altering reaction duration from 1-5 hours, investigated for 16 and 23% wt% BA. 1-hour reaction time shown in green and 5-hour reaction time in orange.

While there was modest improvement of particle size and morphology, measuring the glass transition temperature of the particles revealed important distinctions in seed particle chemistry depending on reaction time. The DSC results indicated a substantial difference in glass transition temperature for the two samples with 23 wt% BA: a 1-hour reaction time resulted in a T_g of 78 °C while the 5-hour reaction time yielded a T_g of 27 °C. The glass transition temperature of a multicomponent polymer can be predicted based on the ratios of the monomers that are used during the synthesis by the Flory-Fox Equation:

$$\frac{w_1}{T_{g1}} + \frac{w_2}{T_{g2}} + \frac{w_3}{T_{g3}} + \frac{w_4}{T_{g4}} = \frac{1}{T_g} \quad \text{w}_\text{n}\text{: Component n weight fraction}$$

This equation was used to predict the T_g of the seed particles prior to synthesis, then the predictions were compared with the measured T_g's found via DSC. The glass transition temperatures of the monomers used vary widely: BA (-53 °C), MMA (105 °C), AMA (54 °C), and MAA (228 °C).

For the 23 wt% BA seed particles, the predicted T_g is -12 °C, which is much closer to the experimental result obtained using a longer reaction time. A T_g of 78 °C for the 1-hour reaction time indicates a higher prevalence of either MMA or MAA in the synthesized particles. Since MMA is present in much higher concentrations than MAA, the discrepancy in T_g is likely due preferential polymerization of MMA at the beginning of the reaction and BA left unreacted. When the reaction is carried out over a longer duration the T_g reduces due to the better incorporation of BA in the final seed particle. The use of the Flory-Fox equation in interpreting this data should be seen as qualitative, since as discussed in Section 3.1.4, it involves limitations and assumptions. However, the conclusions that BA better incorporates into the seed particles in longer reaction times is also supported by other literature on similar systems.

Works by Roos et al. and París et al. have confirmed the greater reactivity of MMA relative to BA and how this can leave BA unreacted for shorter reaction durations.[39,40] A way of quantifying this conclusion within this study would be to do NMR on the synthesized seed particles, however, the presence of allyl methacrylate caused crosslinking into a gel during dissolution in chloroform, preventing liquid state NMR testing. Samples would need to be prepared without allyl methacrylate to see if gelation could be prevented, or solid state NMR would need to be pursued instead. A 5-hour reaction duration was chosen for future experiments to improve incorporation of the BA into the particles. A potential continuation of this work would be to analyze how morphology, T_g, and size of a single sample develop over time. This can be accomplished by taking aliquots from the reactor vessel at set intervals while the reaction takes place. The reaction time could also be extended beyond four hours to more accurately determine the ideal duration.

3.1.3 Total Monomer Weight Percentage

For the use of these particles as precursors to bilobal particles and ultimately in coatings, it is important to reliably produce particles at each stage with the highest yield, therefore the effect of monomer weight percent on the synthesis was examined. A higher monomer weight percentage will correspond to a higher monomer concentration and higher final solids content. The Bohling 2015 procedure calls for a high monomer concentration because the resulting coating is more cost effective, durable, and requires less VOCs during application.[20] Drawbacks of higher monomer concentration are higher viscosity and lower shelf life because the particle are more prone to aggregate.[1]

The total monomer weight percentage is defined as the sum of monomer masses, BA, MMA, AMA, and MAA, relative to the total mass; 38% for the control synthesis, as can be seen in **(Fig. 1)**. The total monomer concentration was varied between 15 and 38 wt%. To maintain the same predicted T_g, the masses of BA, MMA, AMA, and MAA relative to each other were kept constant between the two total monomer weight percentage trials. This is 0.63 and 0.58 BA relative to the total monomers for the two total monomer concentrations **(Fig. 12-13)**. For the samples with 0.63 BA, when monomer concentration was reduced there was no change in the particle size (96 nm) but the PDI increased from 0.07 to 0.18. For the samples with 0.5 BA, size and PDI varied greatly. Higher monomer concentration particle size was 119 nm with a PDI of 0.06 while low monomer concentration particle size was 73 nm with a PDI of 0.18. These results indicate there is no systematic change in particle size/dispersity as a function of monomer weight percent, so future work will use 38 wt % since this is what is more relevant for coatings. A continuation of this study between 20-30 wt% monomer would be of interest to confirm this result. 38% total weight percent monomer was chosen for future experiments.

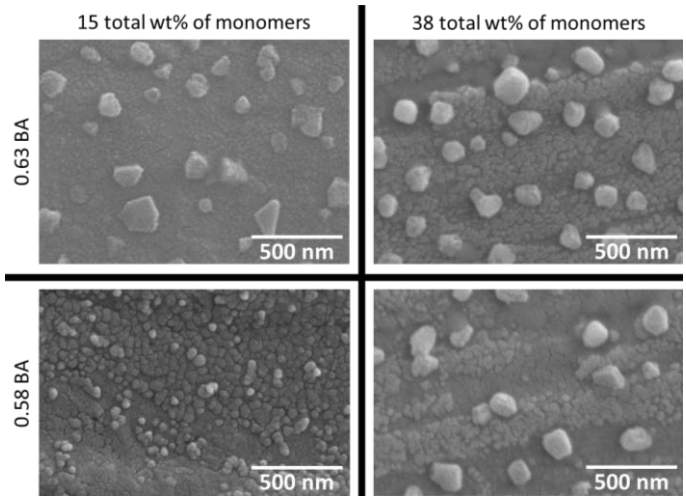

Figure 12: SEM imaging analyzing the effect of altering total monomer weight percentage from 15-38%, investigated for 0.63 and 0.58 BA. These ratios of BA are relative to the total monomer content.

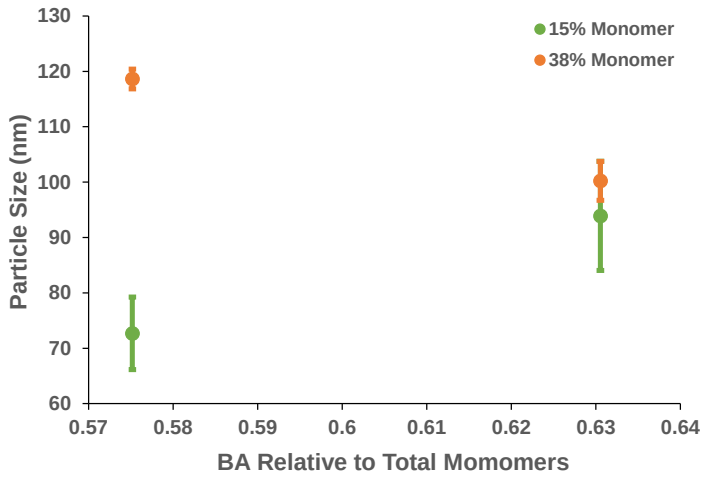

Figure 13: DLS results analyzing the effect of altering total monomer weight percentage from 15-38%, investigated for 0.63 and 0.58 BA. These ratios of BA are relative to the total monomer content. 15 weight percent shown in green and 38 weight percent shown in orange.

3.1.4 Monomer Ratio and Glass Transition Temperature

Motivated by the T_g discrepancies found during the reaction duration testing, the T_g of several samples with varying weight percentages of BA, relative to MMA, were investigated in order to control the seed particle T_g. Controlling seed particle T_g is an important first step in the eventual formulation of bilobal particles with controlled chemistries. In these experiments, the weight percentages of PEM, MAA, and AMA were kept constant at 2, 1, and 1 wt%, respectively, and the overall monomer concentration was kept constant at 38 wt%. Control conditions based on the Bohling et al. 2015 patent were 23 wt% BA, samples were also prepared with 16, 19, and 21 wt% BA.[20] As expected, the measured Tg decreased linearly as the concentration of low-T_g BA was increased **(Fig. 14)**. However, the measured T_g is consistently 12 °C higher than that predicted by the Flory-Fox equation.

The consistent offset between the predicted and measured T_g's may be caused by several different factors. One potential explanation of the shift is that, despite the extended reaction duration, there could still be preferential polymerization of the MMA and only

partial polymerization of the BA. If this is assumed, the actual wt% BA within the particles is less than expected and can be estimated by interpolation of the predicted T_g's. Based on the initial concentrations of 16, 19, 21, and 23 wt% BA, the measured T_g's would indicate that the synthesized particles actually contain 12, 15, 18, and 20 wt% BA, respectively. This would mean at least 10-25% of the BA in the pre-emulsion is left unreacted.

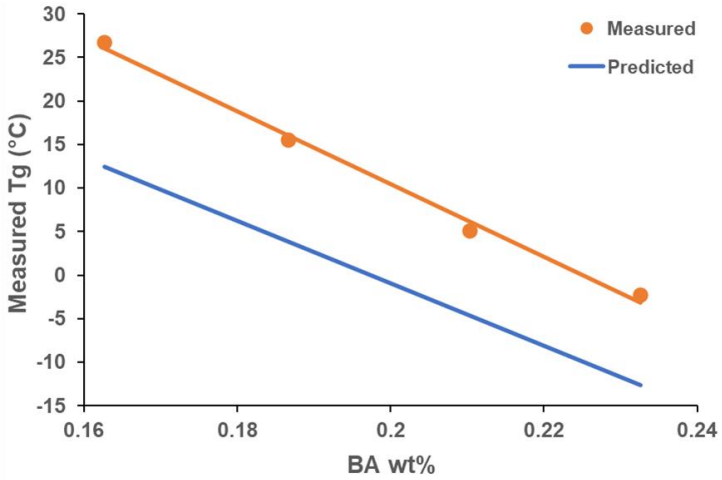

Figure 14: Comparing predicted and measured T_g for 16-23 weight percent butyl acrylate. Predicted T_g's based on the Flory-Fox equation shown in blue and measured T_g found via DSC shown in orange.

The second explanation in the offset in Tg could be due to the assumptions and limitations of the Flory-Fox equation. The Flory-Fox equation does not take into account the effect of the chemical nature or organization of the monomer sub units within the polymer. Several factors that stem from this limitation could account for the shift in predicted versus measured T_g's. The distribution of the monomer sub units can effect overall T_g, this is most apparent in the T_g differences between diblock, gradient, and random copolymers **(Fig. 15)**;[41] the Flory-Fox equation assumes a random copolymer. When there is a significant difference between the reaction rates of the copolymers used, in this case MMA and BA, a gradient copolymer structure is more common.[40] Gradient copolymers have very broad T_g ranges which may impact the clarity of the DSC curves and the resulting accuracy of T_g determination.

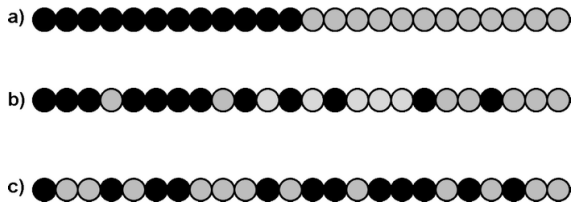

Figure 15: Categories of copolymers from Beginn et al. (a) diblock, (b) gradient, and (c) random.[41]

It is also possible that the method of sample preparation is contributing to the shift. It has been shown that the T_g of polymers in a dried film is substantially higher than while in bulk solution,[42] and the Flory-Fox equation assumes the polymer is in solution. Zhang et al. found that 90 nm diameter polystyrene particles had an increase of 58 °C in a dried state compared to in solution, for larger particles the effect was diminished.[42] This is substantially higher than the 12 °C shift that is observed, however the trend is in the correct direction.

The image quality of the SEM images for seed samples synthesized over the duration of the project have varied considerably. SEM imaging of the samples prepared with 16, 19, 21, and 23 wt% BA can be seen in **(Fig. 16)** and DLS particle size can be seen in **(Fig. 17)**. 23 wt% BA had poor image quality and a higher PDI (>0.07) compared to the other tested ratios. Samples with 21 wt% BA show mild deformation on the SEM slide, but maintain a higher PDI of 0.06 which indicates variability in the size and/or morphology. The PDI of the 16 wt% BA sample was 0.03, however there is an unexplained drop in particle size of ~20 nm when compared to 19 and 21 wt% BA. Taking these factors into consideration, 19 wt% BA is the ideal monomer ratio to achieve monodispersed seeds that do not deform under SEM and DLS. While the samples prepared with 19% BA are ideal for SEM image quality and low PDIs via DLS, this ratio is not necessarily the best for bilobal synthesis or future coating characteristics. Optimal coating characteristics necessitate a low T_g polymer to enable the movement of the particles into a film without high temperature baking. This

could explain the low T_g of the patent, which was predicted to be -12 °C using the Flory-Fox equation and found to be. Samples with 19 wt% BA still have a T_g below room temperature, but the samples with 16 wt% do not.

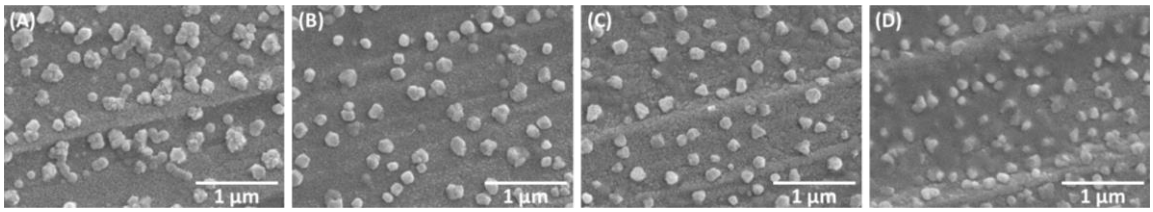

Figure 16: SEM imaging analyzing the effect of altering weight percentage of butyl acrylate: (A) 16 wt% BA (B) 19 wt% BA, (C) 21 wt%, and (D) 23 wt% BA.

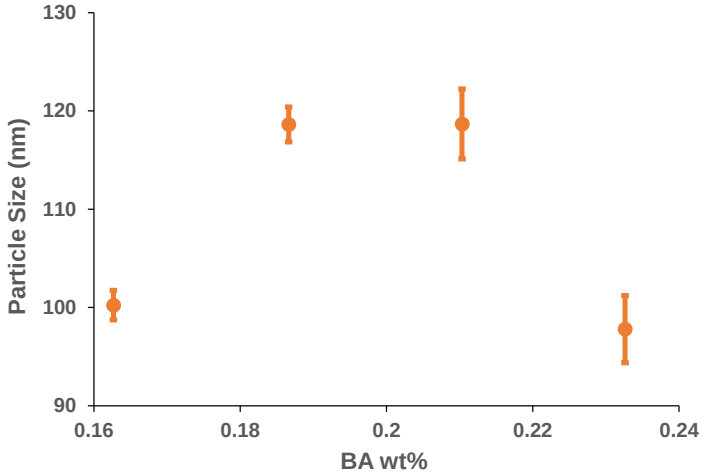

Figure 17: DLS results analyzing the effect of altering weight percentage of butyl acrylate from 16-23%.

The challenge of performing SEM on latex samples is a well-documented problem within the literature, particularly for samples with low T_g's. This is due to the vacuum conditions causing degradation and aggregation of the samples making observation of individual particles challenging.[43] Charging is another common problem for latex because the particles have low conductivity, the beam is deflected often causing low contrast, visual anomalies, and image distortion. The easiest solution to eliminate charging is using a thin layer of gold or platinum to give the sample conductivity, however this will increase particle size and cause rough texturing on the particles and background. 2 nm of gold sputter coating is used for all SEM imaging through-out this work, texturing can be seen

in many of the images as a result. Alternative approaches to prevent degradation, aggregation, and charging often involve staining the particle, cryogenic methods, microtomy, or embedment into a 3D matrix, such as cellulose.[43] Alternative methods of sample preparation could be considered to improve SEM imaging without necessitating an increase in T_g to improve image quality.

3.2 Bilobal Particle Synthesis

The next objective of this project is to use the seed particles synthesized in the previous section and demonstrate proof-of-concept synthesis of bilobal particles. The main variable that was investigated was the monomer/polymer ratio of phase one and phase two. A 40 mL portion of phase one seed particles is used during a second phase polymerization. The seed particles have a ~35% solids content, so this is roughly 14 g of polymer. The phase two monomer pre-emulsion contains 145 g of monomer, resulting in a 1:10 ratio of polymer/monomer between phase one and phase two. The monomers used in phase two are in the same relative concentrations as that used to form the seed particles, with a BA concentration of 26 wt%. It was hypothesized that excessive phase two monomers could cause additional seed particles to form independent of the initial seed particles, reducing the potential yield of bilobal particles. A possibility is that the low yield of bilobal morphology is expected by the Bohling et al. patent, since spherical morphologies still show positive coating characteristics. The high concentration of phase two monomer may be to see an appreciable amount of bilobal morphology.

Samples were prepared with phase ratios of 1:10 and 1:5 using 16 wt% BA seed particles **(Fig. 18)**. Based on an analysis of yield for the SEM images of the particles produced, it can be seen that varying the phase ratio was found to have a negligible effect

on the yield of bilobal particles at this wt% BA **(Fig. 19)**. There is significant debris, most likely the gold sputter coating, which makes identifying particle morphology difficult, particularly for the sample with the 1:5 ratio. TEM generally makes morphology interpretation of the bilobal particles easier, so this should be investigated for the more recent bilobal samples in addition to the SEM imaging.

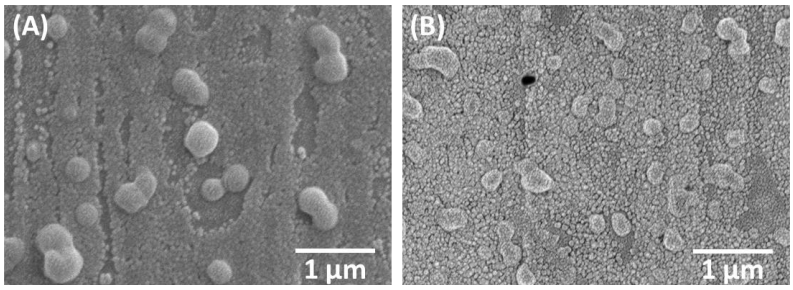

Figure 18: SEM imaging analyzing the effect of altering phase one to phase two ratio from 1:10 to 1:5 (A) 1:10 ratio and (B) 1:5 ratio. Conditions are 5-hour reaction durations and 16 weight percent butyl acrylate in the seed.

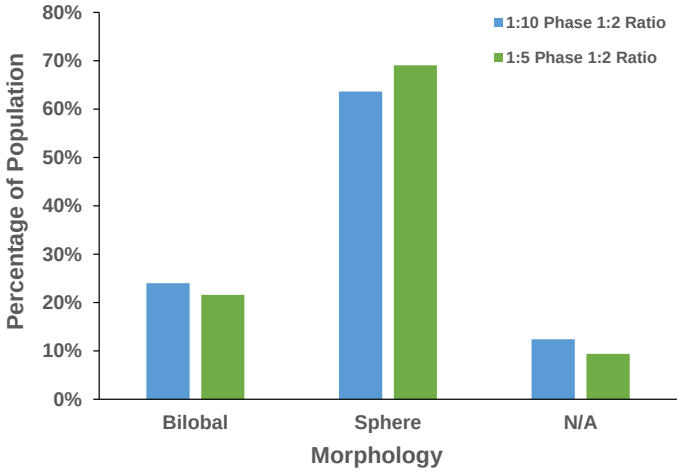

Figure 19: Analyzing the effect of altering phase one to phase two ratio from 1:10 to 1:5 on bilobal particle yield. Conditions are 5-hour reaction durations and 16 weight percent butyl acrylate in the seed.

While reducing the phase ratio successfully made bilobal particles, there were still large quantities of either unreacted seed particles or new spherical particles formed from the phase two monomer. This implies that the concentration of the second phase monomers may need to be reduced further in order to increase the bilobal particle yield. However, if the spherical particles that remain are from unreacted seeds (less likely), higher ratios should be examined. These initial experiments were performed with 16 wt% BA, which

was the highest measured Tg seed particle synthesized with the 5 hour reaction time in the previous section. Repeating this experiment for a higher wt% BA would be of interest to examine how robust the bilobal synthesis is to the chemistry of the seed particles.

(Fig. 20) contains a compilation of preliminary bilobal particles generated with alternative reaction conditions. These experiments were performed before optimizing the reaction duration for seed particle synthesis. Because the seed particles are produced using a 1-hour reaction duration, it is expected that they contain less BA than the 23 wt% expected and more MMA. As discussed previously, the addition of a strong base is what initiates the "blooming of the core," doubling the amount of NaOH was studied to see if it would have a distinguishable impact on the yield of bilobal particles **(Fig. 20b)**. Removing VTMS was considered because it is toxic when inhaled and explicitly stated by the Bohling et al. 2015 patent as an optional reagent **(Fig. 20c)**.[20] These variables were not pursued any further, since the overall yield was not impacted, but these variables could be explored further using the optimized seed particle synthesis.

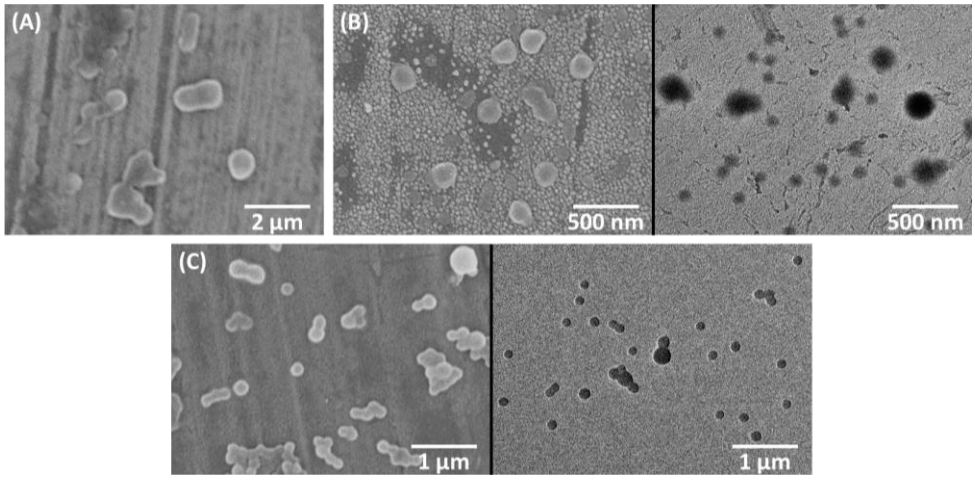

Figure 20: Compilation of preliminary bilobal particles, 1-hour reaction duration and 23 weight percent butyl acrylate, (B) contains double the sodium hydroxide, and (C) contains no vinyltrimethyoxysilane.

The results indicate a similar quantity of bilobal particles as the 5-hour experiments presented above, with significant fractions of aggregates and spherical particles. While the formation of some bilobal particles are promising, it is necessary to further optimize the reaction conditions of the phase two synthesis in order to produce large quantities of bilobal particles with minimal aggregation and unreacted spheres.

It may be beneficial to synthesize seed particles using the phase two monomers independent of the phase one monomers to determine the T_g difference of the two phases. According to work by Misra et al. the harder polymer phase will be drawn to the core and the softer monomer polymer phase to the surface.[21] If the phase one core has too high of a T_g, relative to the second phase shell, it may affect the "blooming of the core." Further investigating 16, 19, 21 wt% BA may improve bilobal particle yield. Once the bilobal synthesis yield is improved, there are several avenues for adding in complexity and functionality to the synthesized particles. As mentioned in section 3.1, HEMA-MM could be investigated as a means to tether crosslinkable functionality to the pendant carboxylic acid groups. To verify the success of this tethering mechanism, HEMA-MM could first be tethered to the initial seed particle independent of the bilobal particles, the tethering could then be verified by NMR.

CHAPTER 4

CONCLUSIONS AND FUTURE WORK

The overarching goal of this thesis was to demonstrate the potential for creating ~100 nm scale acrylic polymer nanoparticles which are stable in aqueous suspension and can be used to create self-stratifying coatings. This was accomplished by building off of the work of Bohling et al. and demonstrating the capability of synthesizing seed particles with controlled glass transition temperature (T_g) to be used in a second stage synthesis to form bilobal particles. Phosphoethyl methacrylate was incorporated into the seed particle phase to act as a representative adhesive functionality. In principle, the adhesive side of the particle would bind to the substrate, and the second lobe would face the environment. Integrating a second distinct orthogonal functionality on the second lobe would enable the self-stratification and present a means to create water-based, self-stratifying, high-performance, acrylic coatings.

Synthesis of the bilobal particles began by optimizing the seed particle precursors. Pre-emulsification yielded less aggregated and more spherical seed particles. We hypothesize that the mixing of surfactant with the polar and non-polar monomers prevents phase separation and encourages uniform polymerization in the reaction chamber. Analyzing the reaction duration gave several insights into optimization of the seed particles as well. Particles formed using a 1-hour reaction duration and those using a 5-hour reaction duration had significantly different T_gs. The differences in the T_g indicated incomplete polymerization of butyl acrylate (BA) and preferential polymerization of methyl methacrylate (MMA), which is in line with the relative reactivities of these monomers. The

total monomer weight percentage was also investigated as a means to reduce incomplete polymerization of the monomers, however the results indicated no systematic change in particle size/dispersity as a function of monomer weight percent. Therefore, seed particles were synthesized at a higher total monomer concentration for use in coating formulations.

The prospect of controlling the particle T_g was investigated by preparing seed particles with a range of BA/MMA concentrations, with the same overall monomer concentration and longer reaction duration. The measured T_gs were compared with predictions based on the Flory-Fox equation. The measured T_g had a persistent offset, ~12 °C higher than expected, however, there is very good qualitative agreement. Given the limitations of the Flory-Fox equation, this trend was promising and the empirical linear trend enables the synthesis of seed particles with the desired T_g based on inputted concentration of BA.

Proof of concept for the second phase polymerization to synthesize bilobal particles was demonstrated, but the yield of the bilobal morphology was ~20%. The ratio of the phase one polymers and the phase two monomers was investigated as a potential means to improve the yield of bilobal morphology. When the ratio was adjusted to reduce the phase two monomers, there were still large quantities of either unreacted seed particles or new spherical particles formed from the phase two monomer. This ratio may need to be reduced further to have an appreciable improvement of bilobal yield.

Opportunities for future work include further optimization of the seed and bilobal particles and expanding the platform into different functionalities. Of the potential options for seed particle optimization, simplifying the pre-emulsion composition should be investigated first. **(Fig. 21)** shows a half factorial design of experiment for additional analysis of the seed particle synthesis; removal of MAA and AMA is considered for 19 and

21% BA. Aliquots taken over the duration of one of the 5-hour reactions would give insights into how the particle distribution and composition develop over time. This could be supplemented by solid-state NMR to gain a better understanding of the seed particle distribution and composition develop over time. The predictive power of the Flory-Fox equation could also be considered further; T_g determination while in a liquid state could be investigated.[42] A final option for optimization of the seed particle is reducing the stir-rate and adding heat during pre-emulsification. This would reduce the monomer droplet surface area without compromising monomer homogeneity and improve particle distribution.[36–38]

Identifier	Variable	Low Level -1	High Level 1
A	MAA	0 g	2.51 g
B	AMA	0 g	1.88 g
C	BA	19 wt%	21 wt%

A	B	C
-1	-1	-1
1	1	-1
-1	1	1
1	-1	1

Figure 21: Proposed design of experiment for seed particle synthesis future work.

Methods of improving the bilobal synthesis should initially focus on the ratio of the phase one and phase two polymers/monomers. A ratio of 1:5 was only investigated for one BA concentration, further reducing the ratio and varying the BA concentration should be considered. Other variables that could be investigated are pre-emulsification of the second phase monomers, the concentration of NaOH, or the T_g of the second phase polymers. Finally, challenges with SEM and TEM imaging should be addressed, degradation and aggregation of the samples make accurate determination of bilobal morphology challenging. Nonetheless, proof of concept bilobal particle formation has been demonstrated and this project represents a powerful start to forming a multi-functional bilobal platform.

REFERENCES

1. Rajaram, S. *Global markets and advanced technologies for paints and coatings*. (2018).
2. Klier, J., Bohling, J. & Keefe, M. Evolution of functional polymer colloids for coatings and other applications. *AIChE J.* **62**, 2238–2247 (2016).
3. Decker, C., Zahouily, K. & Valet, A. Weathering performance of thermoset and photoset acrylate coatings. *J. Coatings Technol.* **74**, 87–92 (2002).
4. Harmsen, A. S., Jansse, P. L., Hoogen, E. & Werf-Willems, N. Crosslinking mechanisms. *Eur. Coatings J.* **49**, 14–19 (2003).
5. Noreen, A., Zia, K. M., Zuber, M., Tabasum, S. & Saif, M. J. Recent trends in environmentally friendly water-borne polyurethane coatings: A review. *Korean J. Chem. Eng.* **33**, 388–400 (2016).
6. Ehnore, J. D., Kincaid, D. S., Komar, P. C. & Nielsen, J. E. Waterborne Epoxy Protective Coatings for Metal Resolution Performance Products LLC*. **74**, 63–72 (2002).
7. Mates, J. E. *et al.* Environmentally-safe and transparent superhydrophobic coatings. *Green Chem.* **18**, 2185–2192 (2016).
8. Lemesle, C. *et al.* Self-stratified bio-based coatings: Formulation and elucidation of critical parameters governing stratification. *Appl. Surf. Sci.* **536**, 147687 (2021).
9. Beaugendre, A. *et al.* Self-stratifying coatings: A review. *Prog. Org. Coatings* **110**, 210–241 (2017).
10. Zhao, J. *et al.* Self-Stratified Antimicrobial Acrylic Coatings via One-Step UV Curing. *ACS Appl. Mater. Interfaces* **7**, 18467–18472 (2015).
11. Yagci, M. B., Bolca, S., Heuts, J. P. A., Ming, W. & de With, G. Self-stratifying antimicrobial polyurethane coatings. *Prog. Org. Coatings* **72**, 305–314 (2011).
12. Van Ooij, W. J., Seth, A., Mugada, T., Pan, G. & Schaefer, D. W. A novel self-priming coating for corrosion protection. *Surf. Eng. - Proc. 3rd Int. Surf. Eng. Conf.* 8–13 (2004).
13. Park, J., Forster, J. D. & Dufresne, E. R. High-Yield Synthesis of Monodisperse Dumbbell-Shaped Polymer Nanoparticles. *J. Am. Chem. Soc.* **132**, 5960–5961 (2010).
14. Kim, J. W. *et al.* Synthesis of Monodisperse Bi-Compartmentalized Amphiphilic Janus Microparticles for Tailored Assembly at the Oil-Water Interface. *Angew. Chemie - Int. Ed.* **55**, 4509–4513 (2016).
15. van Ravensteijn, B. G. P. & Kegel, W. K. Tuning particle geometry of chemically anisotropic dumbbell-shaped colloids. *J. Colloid Interface Sci.* **490**, 462–477 (2017).

16. Bradley, L. C., Stebe, K. J. & Lee, D. Clickable Janus Particles. *J. Am. Chem. Soc.* **138**, 11437–11440 (2016).

17. Chang, F., van Ravensteijn, B. G. P., Lacina, K. S. & Kegel, W. K. Bifunctional Janus Spheres with Chemically Orthogonal Patches. *ACS Macro Lett.* **8**, 714–718 (2019).

18. Stubbs, J. M. & Sundberg, D. C. The dynamics of morphology development in multiphase latex particles. *Prog. Org. Coatings* **61**, 156–165 (2008).

19. Blenner, D., Stubbs, J. & Sundberg, D. Multi-lobed composite polymer nanoparticles prepared by conventional emulsion polymerization. *Polymer (Guildf).* **114**, 54–63 (2017).

20. Bohling, J. C., Brownell, A. S. & Tiwary, Y. Dispersion of Adsorbing Emulsion Polymer Particles. (2015).

21. Misra, A. & Urban, M. W. Acorn-Shape Polymeric Nano-Colloids: Synthesis and Self-Assembled Films. *Macromol. Rapid Commun.* **31**, NA-NA (2009).

22. Limousin, E., Ballard, N. & Asua, J. M. The influence of particle morphology on the structure and mechanical properties of films cast from hybrid latexes. *Prog. Org. Coatings* **129**, 69–76 (2019).

23. Rao, J. P. & Geckeler, K. E. Polymer nanoparticles: Preparation techniques and size-control parameters. *Prog. Polym. Sci.* **36**, 887–913 (2011).

24. Bohling, J. C. *et al.* Pigmented Paint Formulation with a Phosphorus Acid Functionalized Latex Binder and an Associative Thickener. (2017).

25. Rahmani, S. *et al.* Chemically Orthogonal Three-Patch Microparticles. *Angew. Chemie Int. Ed.* **53**, 2332–2338 (2014).

26. Nie, Z., Li, W., Seo, M., Xu, S. & Kumacheva, E. Janus and Ternary Particles Generated by Microfluidic Synthesis: Design, Synthesis, and Self-Assembly. *J. Am. Chem. Soc.* **128**, 9408–9412 (2006).

27. Kaufmann, T. *et al.* Bifunctional Janus beads made by "sandwich" microcontact printing using click chemistry. *J. Mater. Chem.* **22**, 6190 (2012).

28. Gentili, D. & Cavallini, M. Wet-lithographic processing of coordination compounds. *Coord. Chem. Rev.* **257**, 2456–2467 (2013).

29. Eckersley, S. T. & Rudin, A. Film Formation of Acrylic Copolymer Latices: A Model of Stage II Film Formation. in *ACS Symposium Series* vol. 648 2–21 (1996).

30. Jiang, S. *et al.* Design colloidal particle morphology and self-assembly for coating applications. *Chem. Soc. Rev.* **46**, 3792–3807 (2017).

31. Kirillova, A., Marschelke, C., Friedrichs, J., Werner, C. & Synytska, A. Hybrid Hairy Janus Particles as Building Blocks for Antibiofouling Surfaces. *ACS Appl. Mater. Interfaces* **8**, 32591–32603 (2016).

32. Yang, T. *et al.* Dumbbell-Shaped Bi-component Mesoporous Janus Solid Nanoparticles for Biphasic Interface Catalysis. *Angew. Chemie Int. Ed.* **56**, 8459–8463 (2017).

33. Forster, J. D. *et al.* Assembly of Optical-Scale Dumbbells into Dense Photonic Crystals. *ACS Nano* **5**, 6695–6700 (2011).

34. Panczyk, M. M., Park, J.-G., Wagner, N. J. & Furst, E. M. Two-Dimensional Directed Assembly of Dicolloids. *Langmuir* **29**, 75–81 (2013).

35. González, I., Mestach, D., Leiza, J. R. & Asua, J. M. Adhesion enhancement in waterborne acrylic latex binders synthesized with phosphate methacrylate monomers. *Prog. Org. Coatings* **61**, 38–44 (2008).

36. Cui, M., Liu, C., Xu, Q. & Li, R. Effect of hybrid emulsifier (reactive coupling with anionic) on the properties of acrylic emulsion. *J. Adhes. Sci. Technol.* **29**, 1758–1769 (2015).

37. Durbin, D. P., El-Aasser, M. S., Poehlein, G. W. & Vanderhoff, J. W. Influence of monomer preemulsification on formation of particles from monomer drops in emulsion polymerization. *J. Appl. Polym. Sci.* **24**, 703–707 (1979).

38. CHEN, S., JIANG, L. & DAN, Y. Synthesis of Core-Shell Latex Particles Through One-Step Emulsion Polymerization. *J. Macromol. Sci. Part B* **51**, 605–618 (2012).

39. Roos, S. G., Müller, A. H. E. & Matyjaszewski, K. Copolymerization of n -Butyl Acrylate with Methyl Methacrylate and PMMA Macromonomers: Comparison of Reactivity Ratios in Conventional and Atom Transfer Radical Copolymerization. *Macromolecules* **32**, 8331–8335 (1999).

40. París, R. & De la Fuente, J. L. Glass transition temperature of allyl methacrylate-n-butyl acrylate gradient copolymers in dependence on chemical composition and molecular weight. *J. Polym. Sci. Part B Polym. Phys.* **45**, 1845–1855 (2007).

41. Beginn, U. Gradient copolymers. *Colloid Polym. Sci.* **286**, 1465–1474 (2008).

42. Zhang, C., Guo, Y. & Priestley, R. D. Glass Transition Temperature of Polymer Nanoparticles under Soft and Hard Confinement. *Macromolecules* **44**, 4001–4006 (2011).

43. Geng, X., Zhai, M. X., Sun, T. & Meyers, G. Morphology Observation of Latex Particles with Scanning Transmission Electron Microscopy by a Hydroxyethyl Cellulose Embedding Combined with RuO 4 Staining Method. *Microsc. Microanal.* **19**, 319–326 (2013).